




 Cite this: *RSC Adv.*, 2020, 10, 28819

Protein-mediated sponge-like copper sulfide as an ingenious and efficient peroxidase mimic for colorimetric glucose sensing†

 Yan Liu, * Haijia Jin, Wenting Zou and Rong Guo *

Strenuous efforts have been made to develop nanozymes for achieving the performance of natural enzymes to broaden their application in practice, but the fabrication of high-performance and biocompatible nanozymes *via* facile and versatile approaches has always been a great challenge. Here, sponge-like casein-CuS hybrid has been facilely synthesized in the presence of amphiphilic protein-casein through a simple one-step approach. Casein-CuS hybrid exhibits substrates-dependent peroxidase-like activity. Casein-CuS hybrid exhibits well peroxidase-like activity with 3,3',5,5'-tetramethylbenzidine (TMB) and 1,2-diaminobenzene (OPD) as substrates, and the affinity of OPD towards the hybrid nanozyme is much higher than that of TMB. More importantly, due to the high affinity of OPD and the well biocompatibility of the hybrid nanozyme, a superior enzyme cascade for glucose based on the well cooperative effect of casein-CuS hybrid and glucose oxidase is developed. The proposed glucose sensor exhibits a wide linear range of 0.083 to 75 μM and a detection limit of 5 nM. This suggests the promising utilization of protein-metal hybrid nanozymes as robust and potent peroxidase mimics in the medical, food and environmental detection fields.

Received 23rd June 2020

Accepted 29th July 2020

DOI: 10.1039/d0ra05496h

rsc.li/rsc-advances

1. Introduction

As promising alternatives to natural enzymes, nanomaterials with enzyme-like catalytic activity (nanozymes) have attracted wide attention due to their excellent stability, low cost and unique physical-chemical properties of nanomaterials.¹⁻³ The catalytic performances of nanozymes can be modulated easily by changing their composition, morphology and surface microenvironmental properties.⁴⁻⁶ Over the past decade, more and more nanomaterials have been found to display the catalytic activities of natural enzymes, such as peroxidase, oxidase, catalase and superoxide dismutase. Among these nanozymes, peroxidase-mimics have attracted special attention because of its wide application in biological, medical, environmental and food areas.⁷⁻¹⁰ The peroxidase-mimicking nanozyme catalyze the oxidation of substrates such as *o*-phenylenediamine (OPD), 2,2-azino-bis-(3-ethylbenzothiazoline-6-sulfonic acid) (ABTS), and 3,3',5,5'-tetramethylbenzidine (TMB) to the corresponding colored products by H_2O_2 . H_2O_2 is generated in many oxidase, such as glucose oxidase, uricase and cholesterol oxidase, catalyzed reaction, so peroxidase-mimicking nanozymes were developed for colorimetric detection of these metabolites.¹¹⁻¹³

However, the interaction between inorganic nanozymes and natural oxidases may lead to the deactivation of the oxidases, so the detection of these metabolites by using enzyme-like nanomaterials usually involve two-step analytical processes.

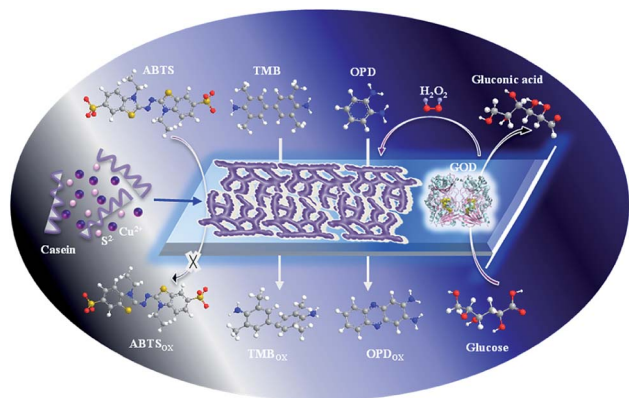
Due to their low toxicity, ease of synthesis, low price and biocompatibility, copper-based nanomaterials based nanozymes have received considerable attraction, but their catalytic activity is still lower than that of natural enzymes.¹⁴⁻¹⁷ Therefore, rationally designing copper-based nanozymes with substantially promoted peroxidase-like activity by controlling the size, shape and surface microenvironment *via* facile and convenient approaches is challenging to broaden their potential application in practice.^{18,19}

Proteins have significant advantages in the synthesis of nanomaterials, such as mild reaction conditions and facile operation processes. In addition, the interaction between proteins and nanomaterials can not only improve their stability, but also enhance their enzymatic activities *via* modifying the surface microenvironment. More importantly, the modified proteins endow nanomaterials with high specific biological recognition, biocompatibility and diversified functions, achieving multifunctional applications of nanomaterials.²⁰⁻²³ Thus, it is extraordinary to design and construct multifunctional copper-nanozymes using proteins with specific structures. Casein, as a natural amphiphilic block copolymer, has not only hydrophilic head group, but also hydrophobic tail group.^{24,25} In our earlier work, metal nanozymes based on casein

School of Chemistry and Chemical Engineering, Yangzhou University, Yangzhou, 225002, Jiangsu, P. R. China. E-mail: yanliu@yzu.edu.cn; guorong@yzu.edu.cn; Fax: +86-514-87971802; Tel: +86-514-87971802

† Electronic supplementary information (ESI) available. See DOI: 10.1039/d0ra05496h





Scheme 1 Schematic illustration of the peroxidase-mimic activity of casein-CuS hybrid and the detection of glucose based on glucose oxidase/casein-CuS hybrid cascade.

have exhibited excellent improved enzyme-like activity and more functionalities.^{26–28}

In this work, the sponge-like casein-CuS hybrid nanozyme with good stability and biocompatibility was prepared *via* one-pot method based on the amphiphilic protein (Scheme 1). The peroxidase-like activity of the hybrid nanozyme displays substrates dependent. Casein-CuS hybrid exhibits well peroxidase-like activity with TMB and OPD as substrates. Contrarily, sponge-like casein-CuS has no peroxidase-like activity with the negatively charged substrate ABTS. Significantly, the enzyme cascade reaction system was constructed based on sponge-like casein-CuS and glucose oxidase, and the one-step method for the detection of glucose was provided. Therefore, a rational designed protein–copper hybrid nanozymes *via* facile and versatile approaches has wide application prospects in many fields such as clinical diagnosis, environmental and drug analysis.

2. Experimental section

2.1. Reagents and chemicals

Casein was purchased from Sigma (>99%). 3,3',5,5'-Tetramethylbenzidine (TMB), *o*-phenylenediamine (OPD) and 2,2'-azinobis(3-ethylbenzthiazoline-6-sulfonic acid)diammonium salt (ABTS) were purchased from Sigma. All other reagents used were of analytical grade from Beijing Company, and ultrapure Millipore water (18.2 M Ω) was used as the solvent. Casein powders were dispersed in basic solution under stirring at 60 °C, and the dispersions were stored at 4 °C overnight to allow complete hydration.

2.2. Instrumentation and characterization

The activity of the enzymes of the samples was measured by ultraviolet-visible (UV-vis) spectrometer (Shimadzu UV-2501). The morphology of the sample was observed by a JEM-2100 transmission electron microscope (TEM) and X-ray photoelectron spectroscopy (XPS) analyses were performed using an ESCALAB 250Xi spectrometer (Thermo Fisher Co., USA) with an

Al X-ray source (1350 eV of photons). Fourier transform infrared (FT-IR) spectra of samples were recorded using FT-IR spectroscopy (Nicolet-740). X-ray diffraction (XRD) was carried out by using an X-ray diffractometer model D8 advance (Bruker) with Cu K α radiation ($\lambda = 1.5418 \text{ \AA}$).

2.3. Preparation of sponge-like copper sulfide

0.5 mL 0.1 M copper sulfate solution was added to casein solution of 0.2 mg mL⁻¹, stirred for 30 minutes at room temperature. Then, 0.25 mL 0.2 M sodium sulfide solution was added to the mixture, and stirred vigorously at 80 °C for 15 min to obtain sponge-like casein-CuS product. Place the product in the refrigerator and keep it in reserve.

2.4. Sponge-like copper sulfide as peroxidase mimetics

To investigate the peroxidase-like activity of the as-prepared sponge-like casein-CuS hybrid, the catalytic oxidation of the peroxidase substrate TMB in the presence of H₂O₂ was tested. In a typical experiment, 45 μ L of 15.0 mM TMB, 20 μ L of the sponge-like casein-CuS stock solution, and 37.5 μ L of 10 M H₂O₂ were added into 2.8975 mL of 0.2 M pH 4.0 acetate buffer at 25 °C. The solution was then transferred for UV-vis scanning after incubating for 20 min.

2.5. Determination of H₂O₂

The casein-CuS hybrid (20 μ L) was introduced into acetate buffer (2.905 mL, pH 4.0), followed by the addition of TMB solution (45 μ L, 15 mM) and 30 μ L of different concentrations of H₂O₂. The mixture was incubated at 25 °C for 20 min with continuous oscillation. The final reaction solution was used to perform absorption spectroscopy measurements.

2.6. Determination of glucose

The prepared casein-CuS hybrid (240 μ L) and 50 μ L of 20 mg mL⁻¹ glucose oxidase was introduced into 2.56 mL 0.2 M pH 4.0 acetate buffer. Then, 100 μ L of 15 mM OPD was added and finally 50 μ L of different concentrations of glucose was added. The reaction was carried out in a water bath at 40 °C for 60 min, and the UV-vis spectrum was measured.

3. Results and discussion

3.1. Characterization of sponge-like copper sulfide

Fig. 1A is the TEM image of the prepared CuS nanomaterials. It can be seen from the image that the prepared sample has a sponge-like structure. Fig. 1B is the XRD spectra of CuS products. The diffraction peaks near 29.24°, 31.75°, 47.98°, 52.54° and 59.05° correspond to the diffraction planes {102}, {103}, {110}, {108} and {116} CuS crystal planes respectively, which are consistent with the JCPDS spectra of the CuS standard (JCPDS card no. 06-0464), indicating the successful synthesis of CuS. The spectrum with low quality may be due to binding of protein. Fig. 1C shows the FTIR spectra of casein and sponge-like casein-CuS. The absorption peak of casein at 1645 cm⁻¹ indicates that casein molecules present disordered

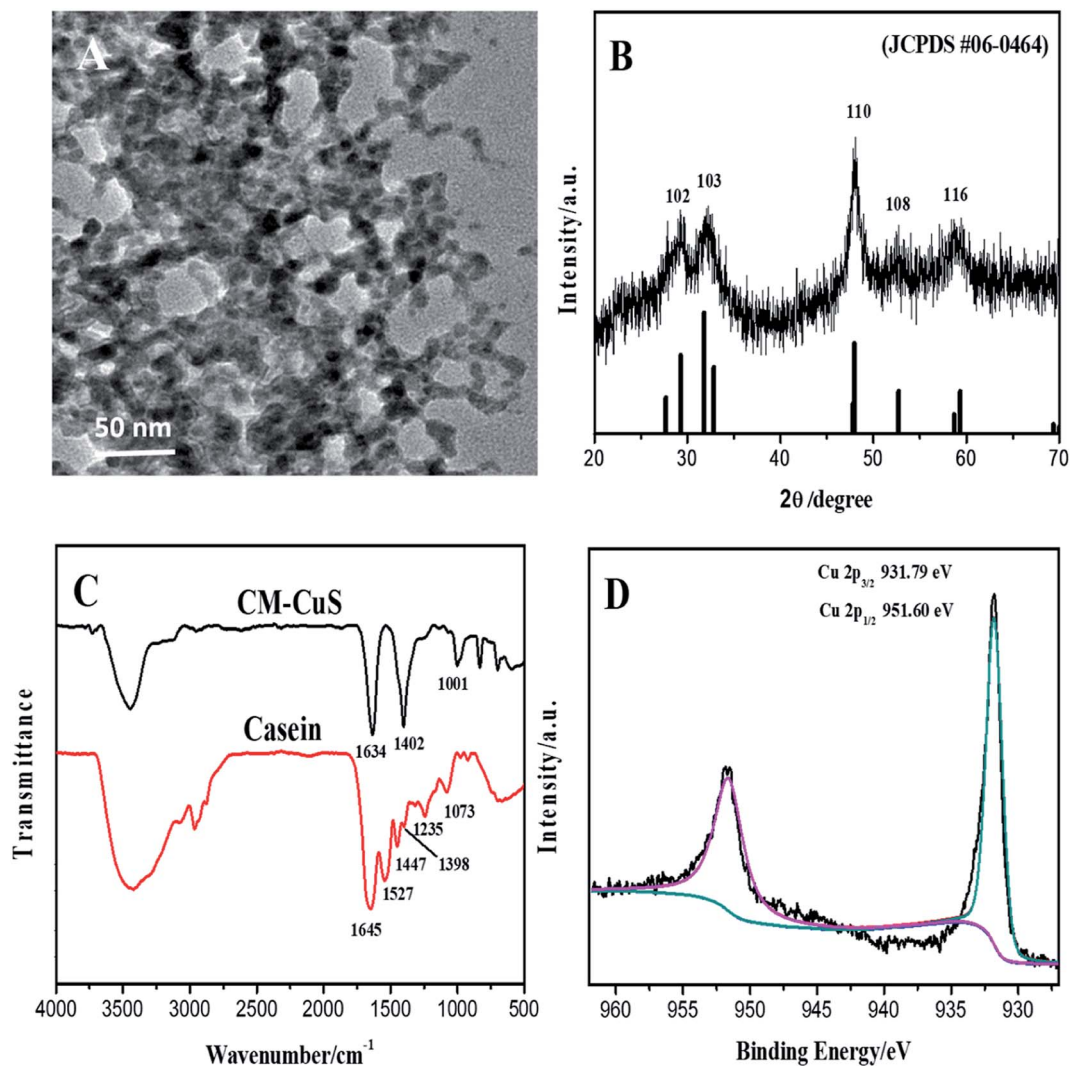


Fig. 1 TEM image (A), XRD spectra (B), FT-IR spectra (C) and high-resolution spectra of Cu 2p spectra (D) of the casein-CuS hybrid.

structure. The FTIR spectrum of sponge-like casein-CuS shows an absorption peak at 1634 cm^{-1} , indicating that the casein chain expanded after binding with CuS. Casein contains about 17% aspartic acid (Asp) and 23% glutamic acid (Glu) residues, and carboxyl functional groups can coordinate with CuS. As expected, the absorption peaks of COO^- on Asp and Glu residues in sponge-like casein-CuS changed significantly at 1447 and 1398 cm^{-1} , so these residues matter much in the formation such sponge-like casein-CuS hybrid.

The XPS spectrum shows the presence of C, O, N, Cu, and S (Fig. S1A†). As shown in Fig. S1B,† the binding energies of $\text{S } 2p_{1/2}$ and $\text{S } 2p_{3/2}$ are 162.55 eV and 161.35 eV , respectively. It can be seen from Fig. 1D that the binding energies of $\text{Cu } 2p_{1/2}$ and $\text{Cu } 2p_{3/2}$ are 951.60 and 931.79 eV , which confirms the formation of CuS. Compared with that of $\text{Cu } 2p_{1/2}$ (952.30 eV) in CuS, the binding energy of casein-CuS hybrid (951.60 eV) is about 0.7 eV lower, which is caused by the electron transfer from proteins to CuS.

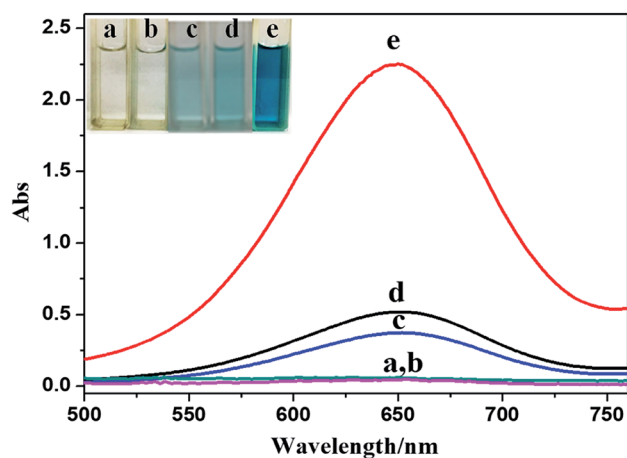


Fig. 2 UV-vis spectra of different systems ((a) TMB + casein-CuS hybrid, (b) TMB + H_2O_2 , (c) TMB + Cu^{2+} + H_2O_2 , (d) TMB + CuS + H_2O_2 , (e) TMB + casein-CuS hybrid + H_2O_2).

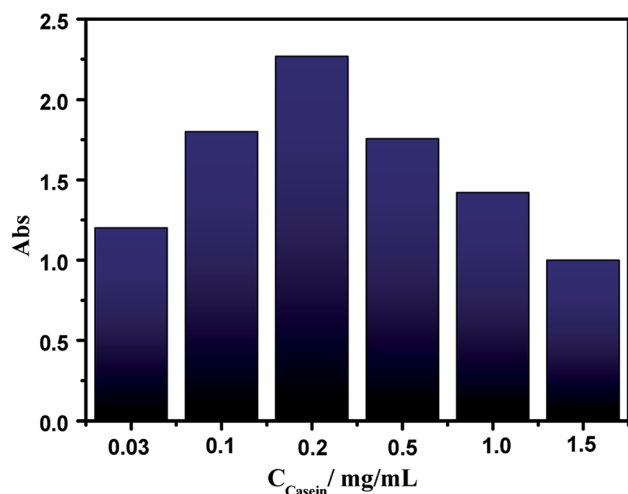


Fig. 3 The peroxidase-like activity of CuS materials prepared in the presence of casein with different concentrations.

3.2. Peroxidase-like activity of sponge-like copper sulfide

TMB is a peroxidase-like (HRP-like) chromogenic substrate. HRP can catalyze the oxidation of TMB by hydrogen peroxide and the absorption peak of the oxidation product appears at 652 nm. Fig. 2 shows the UV-vis spectra of different systems. It can be seen from the figure that sponge-like casein-CuS can catalyze the oxidation of TMB by hydrogen peroxide to produce blue products quickly. There is much difference in the

absorbance of the systems without the hybrid nanozyme or H₂O₂ at 652 nm. This indicates that sponge-like casein-CuS and hydrogen peroxide are necessary for the reaction. In addition, Cu²⁺ and bare CuS (bare CuS was synthesized without protein) catalyze the oxidation of TMB by hydrogen peroxide very weakly. Thus, the high HRP-like activity was related to the structure and surface microenvironment of the sponge-like casein-CuS.

It is noteworthy that the protein concentration is very important to obtain sponge-like casein-CuS hybrid with high HRP-like activity. Fig. 3 shows the activity of CuS synthesized under different casein concentration. With the increase of casein concentration, the activity of CuS first increases and then decreases, and reaches the highest when casein concentration is 0.2 mg mL⁻¹. Fig. 4 show the TEM images of CuS materials synthesized under different casein concentration. It can be seen that CuS is random nanoparticle aggregates synthesized under low protein concentration. Then, sponge-like structure forms with the increase of casein concentration. Sponge-like structure gradually disappears and transforms into CuS nanoparticles with the further increase of casein concentration. Thus, the excellent catalytic performance of the casein-CuS hybrid is due to the sponge-like structure and surface microenvironment.

Similar to other nanozymes, changes in temperature and pH affect the catalytic activity of casein-CuS hybrid. As shown in Fig. 5A, as the reaction temperature increases, the activity first increases and then decreases. When the temperature is 25 °C, the catalytic activity reaches the maximum. Therefore, the reaction temperature was chosen to be 25 °C for further

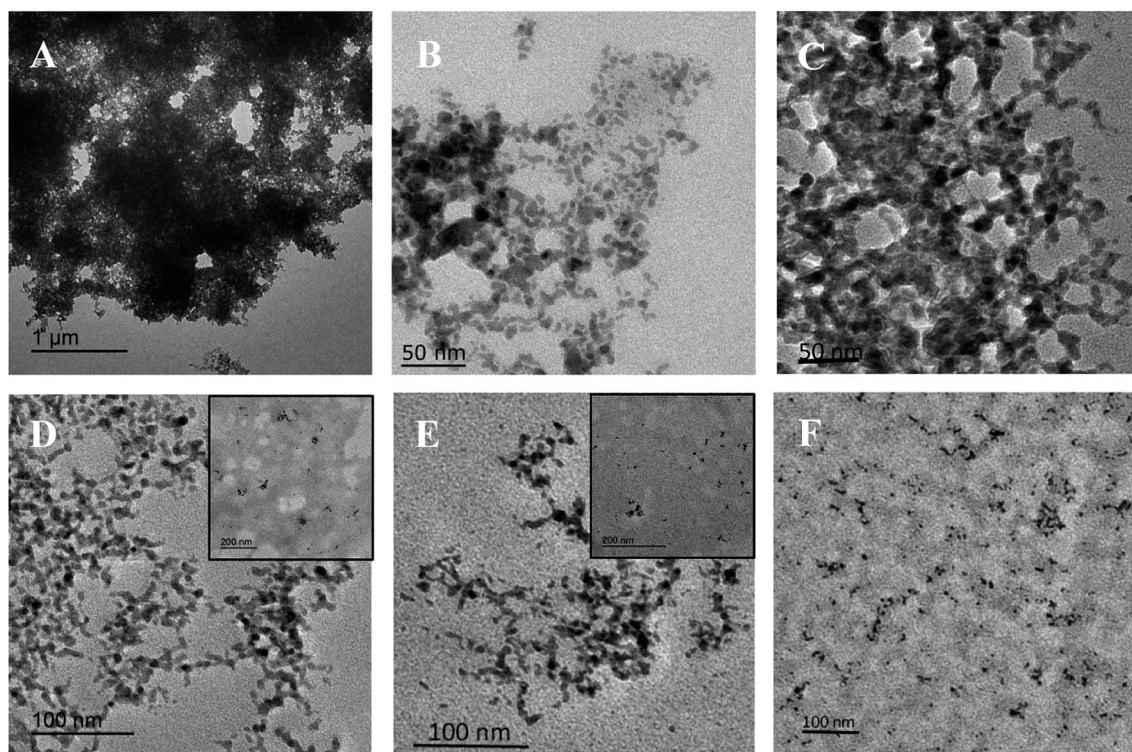


Fig. 4 TEM images of CuS materials prepared in the presence of casein with different concentrations. The concentration of casein is 0.03 (A), 0.1 (B), 0.2 (C), 0.5 (D), 1.0 (E) and 1.5 (F) mg mL⁻¹.

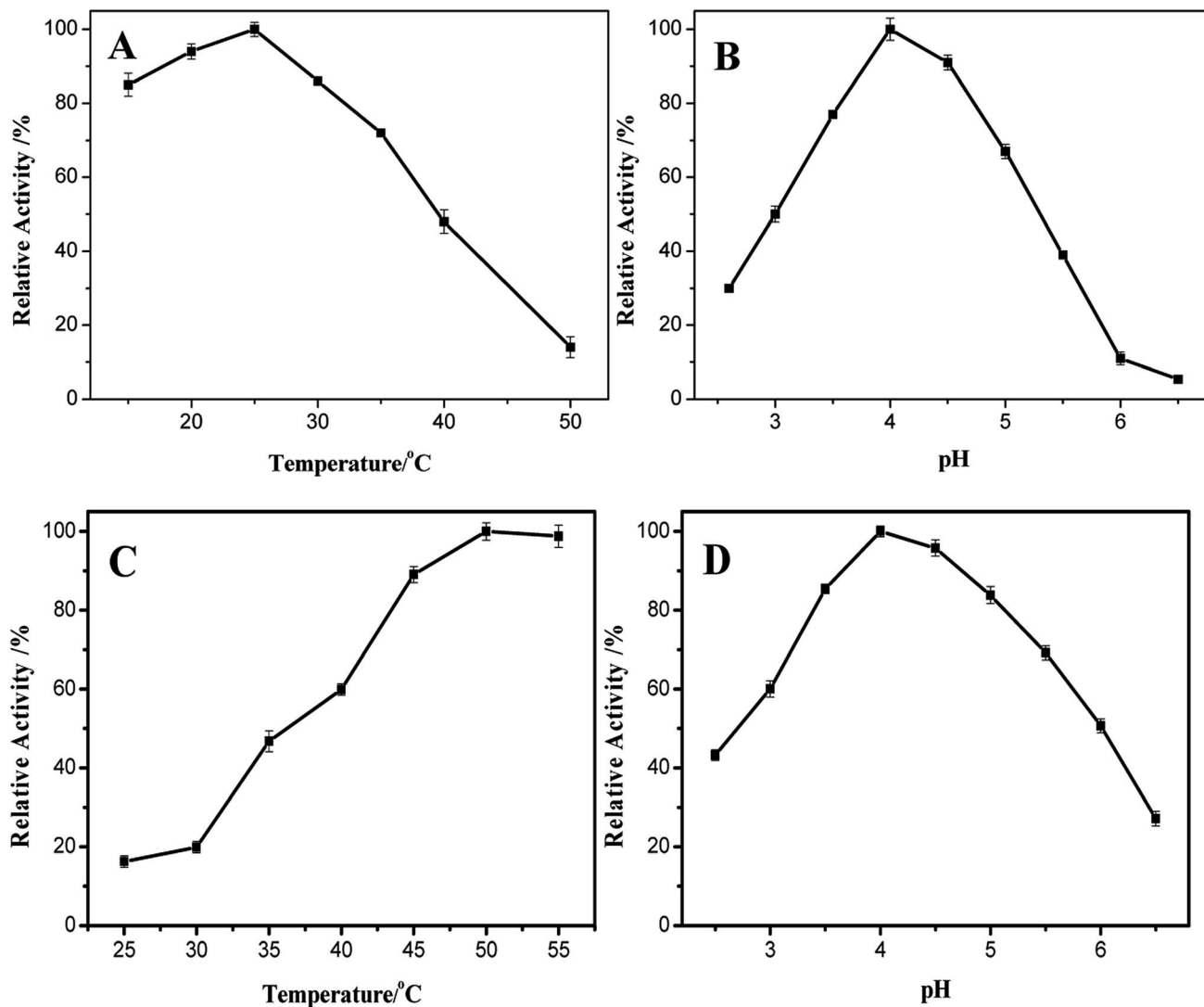


Fig. 5 Effect of temperature (A and C) and pH (B and D) on the peroxidase-like activity of sponge-like casein-CuS with TMB (A and B) and OPD (C and D) as the substrate.

experiments. Moreover, the enzymatic activity of the casein-modified sponge-like casein-CuS did not change much between 15 and 30 °C, indicating that the sponge-like casein-CuS can be applied in the room temperature range well. Solution pH is an important factor affecting the catalytic activity of sponge-like casein-CuS in the sensing system, and the optimum pH is 4.0 as shown in Fig. 5B.

The peroxidase-like activity of the sponge-like casein-CuS hybrid can be further evaluated by determining the kinetic parameters using the initial rate method of steady state kinetics. According to Lineweaver-Burk plot, Michaelis-Menten constant (K_m) and maximum initial velocity (V_{max}) were obtained. As shown in Table S1,† K_m values for TMB and H_2O_2 are 0.355 and 234 mM, indicating the hybrid nanozymes have a stronger affinity for TMB and a weaker affinity for H_2O_2 . This is consistent with many earlier metallic oxide based nanozymes. The maximum reaction rates of both TMB and H_2O_2 are greater than HRP, which may be closely related to the sponge-like

structure of casein-CuS hybrid and the surface microenvironment provided by proteins. For the peroxidase-mimicking activity of the nanozymes, hydroxyl radicals (OH^\bullet) is usually produced in the catalytic process. The fluorescence probe terphthalic acid (TA) was used to confirm the formation of OH^\bullet since it can capture OH^\bullet to form a fluorescent hydroxyterphthalate (TAOH). As shown in Fig. S4,† TA reacts with H_2O_2 to produce the product with a fluorescent peak at about 450 nm, demonstrating the formation of OH^\bullet in the catalytic process.

In order to fully understand the HRP-like activity of sponge-like casein-CuS, ABTS and OPD were selected as the substrates (Fig. 6A and B). The sponge-like casein-CuS exhibits very low peroxidase-like activity with ABTS as a substrate but outstanding peroxidase-like activity with OPD as a substrate. The sponge-like copper sulfide exhibits low catalytic activity with ABTS as a substrate, which may be due to the negative charged protein on the surface of casein-CuS hybrid. The repulsion reduces the affinity of ABTS towards the hybrid

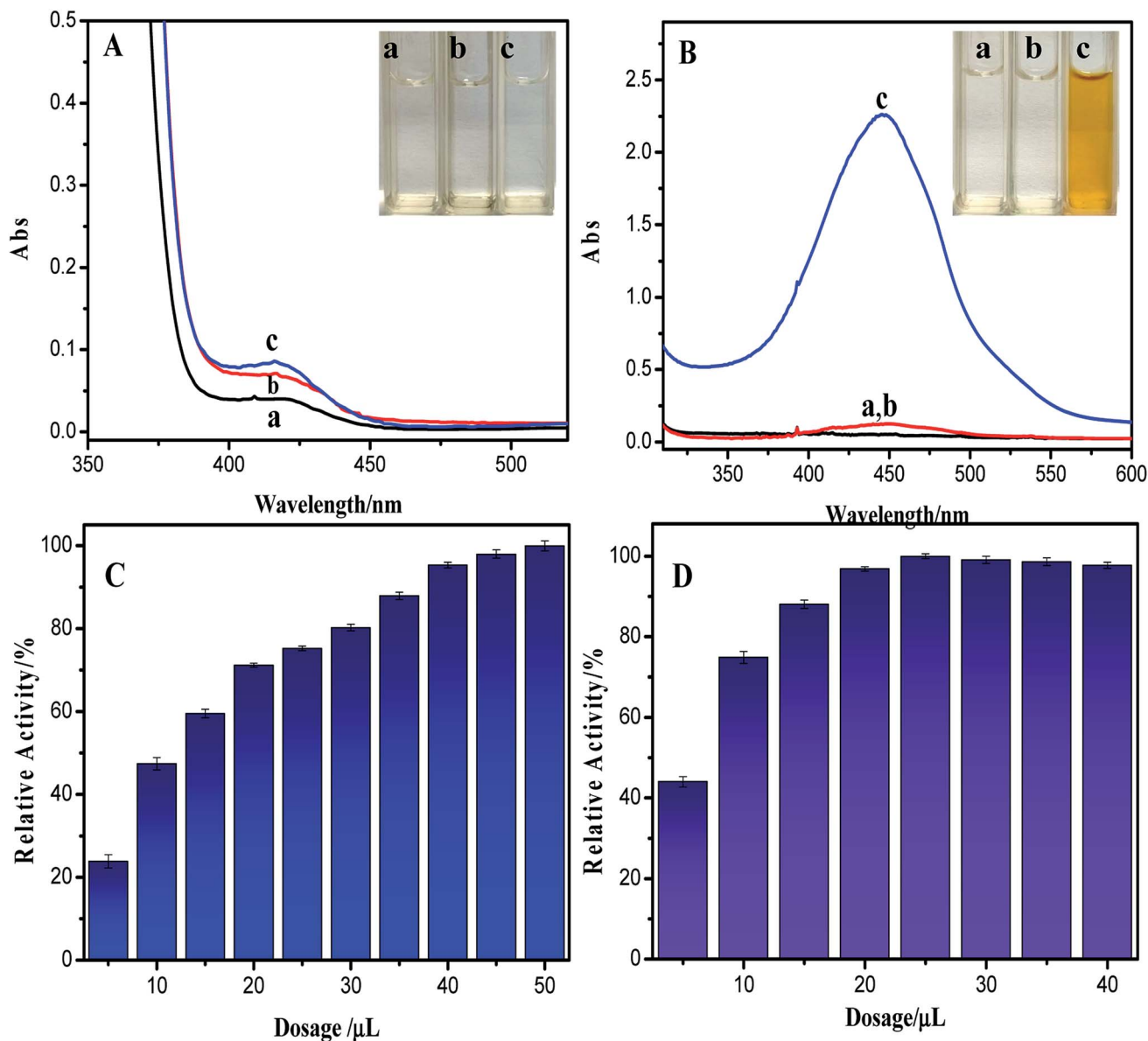


Fig. 6 UV-vis spectra of different systems for ABTS (A) and OPD (B) ((a) ABTS/OPD + casein-CuS hybrid, (b) ABTS/OPD + H₂O₂, (c) ABTS/OPD + casein-CuS hybrid + H₂O₂). Effect of the dosage of the hybrid nanozyme on the peroxidase-like activity of the hybrid nanozyme with TMB (C) and OPD (D) as substrates.

nanozyme. At the same time, we also studied the effect of different conditions on the enzyme activity of sponge-like casein-CuS with OPD as the substrate. As can be seen from Fig. 5C and D, the optimum temperature and pH value are 50 °C and pH = 4.0, respectively. As is well-known, the enzyme-like activity of nanozyme depends much on its size, shape and surface microenvironment. In addition, the enzyme-like activity of nanozymes is also influenced by the intrinsic property of the substrate used. Here, the two substrates have distinct interaction with the nanozyme due to their intrinsic structure of the two substrates, which is confirmed by the different affinity towards nanozymes (K_m). Thus, the different optimal conditions for TMB and OPD as substrates may be due to their distinct interaction with the nanozyme.

For comparison, K_m and V_{max} of casein-CuS hybrid with OPD and H₂O₂ as substrates were obtained by the Lineweaver-Burk linear equation (Table S2†). As can be seen from Table S2,† when OPD is used as a substrate, the K_m values of the sponge-like casein-CuS with the substrates OPD and H₂O₂ are 0.031 mM and 6.78 mM, which are much smaller than that with TMB as the substrate. Thus, compared with TMB as the substrate, OPD and H₂O₂ have much higher affinity towards the hybrid nanozymes. Fig. 6C and D shows the effect of dosages of sponge-like casein-CuS hybrid on the peroxidase-like activity of the hybrid nanozyme with TMB and OPD as substrates. It can be seen from Fig. 6 that the activity of the hybrid with TMB as the substrate has been increasing slowly with the increases of the dosages of the hybrid nanozyme used. However, the catalytic

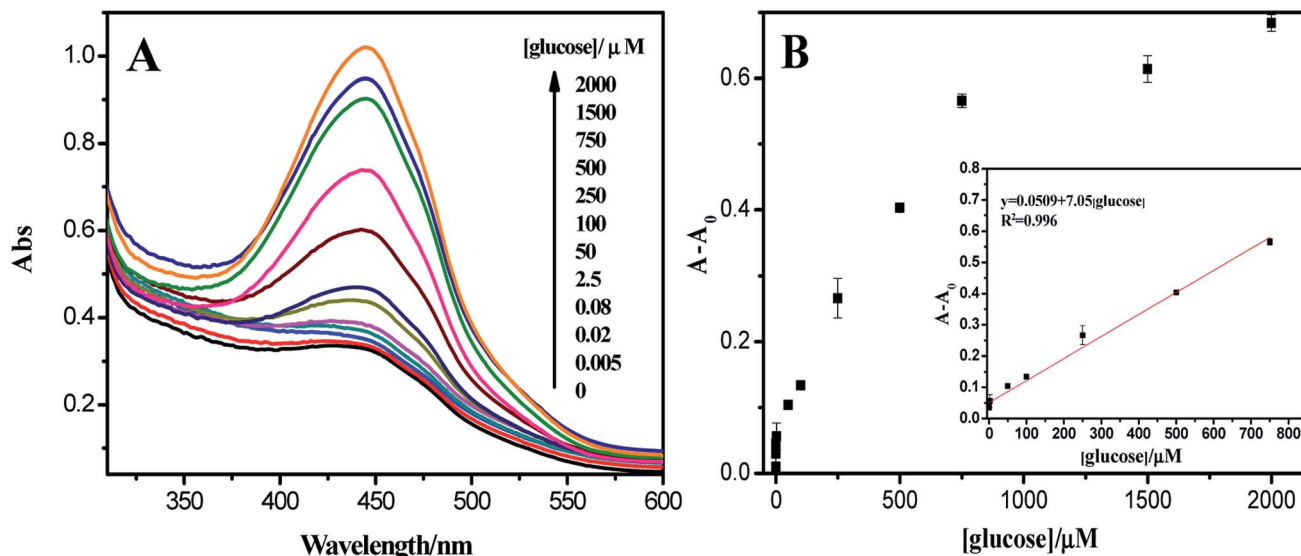


Fig. 7 (A) UV-vis spectra of TMB oxidation catalyzed by GOD/casein-CuS hybrid at different glucose concentrations. (B) The relationship between the concentration of glucose and absorbance change.

activity of the hybrid with OPD as the substrate reaches 90% of the highest activity when 15 μL of the hybrid was added. This further indicates the high affinity of OPD towards the hybrid nanozyme.

3.3. Colorimetric detection of glucose

The catalytic activity of sponge-like casein-CuS hybrid is related to the concentration of hydrogen peroxide, and hydrogen peroxide is the main product of glucose oxidation catalyzed by glucose oxidase (GOD). Therefore, sponge-like casein-CuS can further be used to detect glucose. Glucose detection with nanozymes usually involves two steps. Firstly, GOD oxidizes glucose to produce hydrogen peroxide under neutral conditions, and then nanozymes catalyze the oxidation of substrates by hydrogen peroxide to produce colored oxidized substrate under acidic conditions. However, the experimental process is somewhat cumbersome and limited in practical application.

Due to the high affinity of OPD towards the hybrid nanozyme, glucose detection can be performed by directly mixing

GOD and casein-CuS hybrid together with OPD as a substrate, and different concentrations of glucose were added to monitor the changes of substrate absorbance. As shown in Fig. 7A, the absorbance at 450 nm gradually increases with the increase of glucose concentration, so glucose can be detected by this method. Notably, there is absorbance of OPD without the addition of glucose, which is due to the OPD substrate oxidized by oxygen when the dosage of casein-CuS hybrid is high. To eliminate this interference, absorbance change of $A - A_0$ was used to detect the glucose concentration. As shown in Fig. 7B, there is a good linear relationship between the absorbance change and the concentration of glucose between 0.083 and 750 μM . The detection limit of glucose ($S/N = 3$) was 5 nM. In order to compare with other nanozymes, the detection limits and linear ranges of different sensors for glucose detection are listed (Table 1). Compared with other methods, this method has high sensitivity, low detection limit and simple operation.

In addition, we also analyzed the selectivity of glucose in the method. Under the optimum conditions, other sugars including

Table 1 Comparison of the performance of different nanomaterials mimetic enzymes for the detection of glucose

Glucose sensing system	Liner range (μM)	Detection limit (μM)	Step	Reference
ZnFe ₂ O ₄ -CNT	0.8–250	0.58	Two	29
Co ₄ N NWs	1–25	0.23	Two	30
3D graphene/Fe ₃ O ₄ -AuNP	0.015–0.50	0.012	Two	31
Si-dots	0.17–200	0.05	Two	32
3D GH-5	5–500	0.8	Two	33
Zn-CuO	25–500	1.5	Two	34
Pt NCs	0–200	0.28	Two	35
ZnFe ₂ O ₄	1.25–18.75	0.3	Two	36
Co ₃ O ₄ -CeO ₂	5–1500	0.21	One	37
Casein-CuS	0.083–750	0.005	One	This work

10 mM fructose, lactose and maltose were investigated. As can be seen from Fig. S5,† sponge-like casein-CuS hybrid has high selectivity for glucose. To confirm the utility of the sensor in practice, it was used to analyze glucose levels in human serum. In the absence of any pretreatment, serum samples were injected instead of glucose. The results using the present method are in good agreement with the values obtained from a local hospital (Table S3†). Therefore, the sensor shows excellent potential in clinical applications for monitoring glucose.

4. Conclusions

Based on amphiphilic proteins, sponge-like casein-CuS hybrid nanozyme was prepared by a simple one-step method. Casein-CuS hybrid can effectively catalyze hydrogen peroxide oxidation of TMB and OPD, but has no catalytic activity for negative charge substrate molecule ABTS, displaying selectivity for substrates. The affinity of OPD towards the hybrid nanozymes is much higher than that of TMB. More importantly, due to the well cooperative effect of casein-CuS hybrid and glucose oxidase, a high-performance enzyme cascade bioplatforM for glucose with a wide linear range of 0.083 to 750 μM and a detection limit of 5 nM for glucose is developed with OPD as the substrate.

Conflicts of interest

There are no conflicts to declare.

Acknowledgements

This work was supported by the National Nature Science Foundations of China (21573190), PAPD and Nature Science Key Basic Research of Jiangsu Province for Higher Education (15KJA150009).

Notes and references

- 1 H. Wei and E. K. Wang, *Chem. Soc. Rev.*, 2013, **42**, 6060–6093.
- 2 L. Z. Gao, J. Zhuang, L. Nie, J. B. Zhang, Y. Zhang, N. Gu, T. H. Wang, J. Feng, D. L. Yang, S. Perrett and X. Y. Yan, *Nat. Nanotechnol.*, 2007, **2**, 577–583.
- 3 Y. Y. Huang, J. S. Ren and X. G. Qu, *Chem. Rev.*, 2019, **119**, 4357–4412.
- 4 A. Ghosh, S. Basak, B. H. Wunsch, R. Kumar and F. Stellacci, *Angew. Chem., Int. Ed.*, 2011, **50**, 7900–7905.
- 5 N. Puvvada, P. K. Panigrahi, D. Mandal and A. Pathak, *RSC Adv.*, 2012, **2**, 3270–3273.
- 6 K. L. Fan, H. Wang, J. Q. Xi, Q. Liu, X. Meng, D. M Duan, L. Z. Gao and X. Y. Yan, *Chem. Commun.*, 2017, **53**, 424–427.
- 7 J. E. Yang, Y. X. Lu, F. Y. Wang, W. J. Jing, S. C. Zhang and Y. Y. Liu, *Sens. Actuators, A*, 2017, **245**, 66–73.
- 8 W. J. Luo, C. F. Zhu, S. Su, D. Li, Y. He, Q. Huang and C. H. Fan, *ACS Nano*, 2010, **4**, 7451–7458.
- 9 J. Zhao, X. Cai, W. Gao and L. L. Zhang, *ACS Appl. Mater. Interfaces*, 2018, **10**, 26108–26117.
- 10 C. Q. Jin, J. J. Lian and Y. Gao, *ACS Sustainable Chem. Eng.*, 2019, **7**, 13989–13998.
- 11 Y. N. Ding, H. Liu, L. N. Gao, X. X. Zhang, Q. Y. Liu and R. C. Zeng, *J. Alloys Compd.*, 2019, **785**, 1189–1197.
- 12 X. H. Chen, S. Han, N. Li, J. J. Lian, Y. X. Zhang, Q. Y. Liu, X. X. Zhang and X. Zhang, *Talanta*, 2020, **218**, 121142.
- 13 J. Yang, Y. Cao, J. Li, M. Lu, Z. Jiang and X. Hu, *ACS Appl. Mater. Interfaces*, 2016, **8**, 12031–12038.
- 14 X. M. Shen, W. Q. Liu, X. J. Gao, Z. H. Lu, X. C. Wu and X. F. Gao, *J. Am. Chem. Soc.*, 2015, **137**, 15882–15891.
- 15 K. L. Wu, W. K. Li, S. Zhang, W. Chen and X. X. Zhu, *Colloids Surf., A*, 2020, **602**, 125063.
- 16 P. Singh, P. Nath, R. K. Arun, S. Mandala and N. Chanda, *RSC Adv.*, 2016, **6**, 92729–92738.
- 17 Y. F. He, X. H. Niu, L. H. Li, X. Li, W. C. Zhang, H. L. Zhao, M. B. Lan, J. M. Pan and X. F. Zhang, *ACS Appl. Mater. Interfaces*, 2018, **1**, 2397–2405.
- 18 Y. He, N. Li, J. Lian, Z. Yang, Z. Liu, Q. Liu, X. Zhang and X. Zhang, *Colloids Surf., A*, 2020, **598**, 124855.
- 19 D. Mott, J. Galkowski, L. Y. Wang, J. Luo and C. J. Zhong, *Langmuir*, 2007, **23**, 5740–5745.
- 20 K. Biswas and N. R. Rao, *ACS Appl. Mater. Interfaces*, 2009, **1**, 811–813.
- 21 S. Wang, W. Chen, L. Hong and X. H. Lin, *ChemPhysChem*, 2012, **13**, 1199–1204.
- 22 W. Zhang, X. Liu, D. Walsh, S. Yao, Y. Kou and D. Ma, *Small*, 2012, **8**, 2948–2953.
- 23 L. Gao, M. Q. Liu, G. F. Ma, Y. L. Wang, L. N. Zhao, Q. Yuan, F. P. Gao, R. Liu, J. Zhai, Z. F. Chai, Y. L. Zhao and X. Y. Gao, *ACS Nano*, 2015, **9**, 10979–10990.
- 24 S. G. Anema and C. G. D. Kruif, *Biomacromolecules*, 2011, **12**, 3970–3976.
- 25 T. Turovsky, R. Khalfin, S. Kababya, A. Schmidt, Y. Barenholz and D. Danino, *Langmuir*, 2015, **31**, 7183–7192.
- 26 Y. Liu, Y. L. Zheng, Z. Chen, Y. L. Qin and R. Guo, *Small*, 2019, **15**, 1804987.
- 27 Y. Liu, Y. P. Xiang, D. Ding and R. Guo, *RSC Adv.*, 2016, **6**, 112435–112444.
- 28 Y. Liu, Y. L. Zheng, D. Ding and R. Guo, *Langmuir*, 2017, **33**, 13811–13820.
- 29 Y. Z. Li, T. T. Li, W. Chen and Y. Y. Song, *ACS Appl. Mater. Interfaces*, 2017, **9**, 29881–29888.
- 30 F. Yuan, H. Zhao and H. Zang, *ACS Appl. Mater. Interfaces*, 2016, **8**, 9855–9864.
- 31 C. K. Wang, J. Y. Li, R. Tan, Q. Q. Wang and Z. X. Zhang, *Analyst*, 2019, **144**, 1831–1839.
- 32 Q. Chen, M. Liu and J. Zhao, *Chem. Commun.*, 2014, **50**, 6771–6774.
- 33 Q. Wang, X. Zhang and L. Huang, *ACS Appl. Mater. Interfaces*, 2017, **9**, 7465–7471.
- 34 A. P. Nagvenkar and A. Gedanken, *ACS Appl. Mater. Interfaces*, 2016, **8**, 22301–22308.
- 35 L. Jin, Z. Meng and Y. Zhang, *ACS Appl. Mater. Interfaces*, 2017, **9**, 10027–10033.
- 36 L. Su, J. Feng and X. Zhou, *Anal. Chem.*, 2012, **84**, 5753–5758.
- 37 N. Alizadeh, A. Salimia and R. Halla, *Sens. Actuators, B*, 2019, **288**, 44–52.